Metalloporphyrin hosts for supramolecular chemistry of fullerenes

Kentaro Tashiro* and Takuzo Aida*

Received 12th October 2006
First published as an Advance Article on the web 5th December 2006
DOI: 10.1039/b614883m

This paper is a *tutorial review* of the host–guest chemistry of fullerenes and metalloporphyrin. Among various host molecules for fullerenes, cyclic hosts composed of metalloporphyrin moieties possess one of the highest affinities toward fullerenes, which can be widely tuned simply by changing the central metal ions of the porphyrin moieties. Inclusion of fullerenes occurs not only by van der Waals interactions but also, in some cases, *via* π-electronic charge-transfer from the host metalloporphyrin moieties to the guest fullerenes. Fullerenes such as C_{120}, upon inclusion with cyclic metalloporphyrin dimers, show an oscillatory motion within the host cavity, whose frequency reflects the solvation/desolvation dynamics of the fullerenes. A molecularly engineered metalloporphyrin host with a self-assembling capability allows a guest-directed formation of a supramolecular peapod, where included fullerenes, as peas, are aligned along the self-assembled metalloporphyrin nanotube, as a pod. Furthermore, certain metalloporphyrin hosts are applicable to the selective extraction of low-abundance higher fullerenes from an industrial production source and also allow spectroscopic discrimination of chiral fullerenes.

Introduction

Host molecules for trapping fullerenes (Chart 1) are of great importance because of their potential application to the extraction, solubilization and chemical modifications of fullerenes.[1] In particular, inclusion of fullerenes *via* π-electronic interactions is highly interesting in view of the supramolecular modulation of the electronic properties of fullerenes. Along this line, cyclic oligomers consisting of electron-rich aromatic components, such as calixarenes, resorcinarenes and cyclotriveratrylenes, have been reported as π-hosts for fullerenes.[1,2] However, the association constants of these host molecules with fullerenes are in the range of 10^4 M^{-1} and are not sufficiently high. Since naphthalene is a better solvent than benzene for fullerenes,[3] one may expect higher affinities for π-extended, larger aromatics toward fullerenes. Metalloporphyrins, which are some of the most extensively studied π-electronic molecules, are composed of an 18-electron, large π-conjugated system[4] and can be considered attractive components for the design of host molecules for fullerenes. While fullerenes usually behave as π-acceptors, metalloporphyrins

---

Department of Chemistry and Biotechnology, School of Engineering, The University of Tokyo, 7-3-1 Hongo, Bunkyo-ku, Tokyo 113-8656, Japan. E-mail: aida@macro.t.u-tokyo.ac.jp; tashiro@macro.t.u-tokyo.ac.jp; Fax: +81-3-5841-7310; Tel: +81-3-5841-7251

Kentaro Tashiro

Dr Kentaro Tashiro was born in 1972 and obtained a PhD in Organic Chemistry in 2000 under the direction of Professor Takuzo Aida at the University of Tokyo. He then began an academic career at the University of Tokyo as a research associate, and is now studying the supramolecular chemistry of largely π-conjugated molecules such as metalloporphyrins and fullerenes. His research interests include (1) supramolecular chemistry of metalloporphyrins and fullerenes and (2) study and application of π-electronic interactions between largely π-conjugated molecules for materials engineering.

Takuzo Aida

Dr Takuzo Aida was born in 1956. He received a BS degree in Physical Chemistry from Yokohama National University in 1979 and a PhD in Polymer Chemistry from the University of Tokyo in 1984. He then began an academic career at the same university, and was involved until 1994 in precision polymer synthesis with metalloporphyrin complexes. In 1996, he was promoted to Full Professor of the Department of Chemistry and Biotechnology, School of Engineering, the University of Tokyo. His research interests include (1) electronic and optoelectronic soft materials, (2) bioinspired dendritic macromolecules, (3) molecular and biomolecular machines and (4) bio-related molecular recognition and catalysis. He is now the project leader of the ERATO-SORST program on "NANOSPACE". He has received many awards including the Wiley Polymer Chemistry Award, IBM Science Award, Nagoya Medal Seminar Award Silver Medal, Tokyo Techno Forum Gold Medal, Arthur K. Doolittle Award and Inoue Prize for Science.

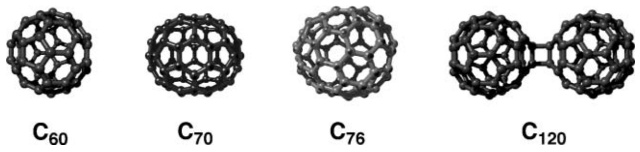

Chart 1 Schematic molecular structures of selected fullerenes.

tend to act as π-donors. Such complementary features are expedient for the interactions between these two π-electronic components. In fact, several co-crystals between metalloporphyrins and fullerenes have been reported, where the fullerene–metalloporphyrin separations are smaller than that of the graphene layers in graphite.[5] However, in solution, the interactions between metalloporphyrins and fullerenes are so weak that they can hardly be visualized spectroscopically unless metalloporphyrins and fullerenes are covalently linked with one another.[6]

We happened to notice that a cyclic dimer of a zinc porphyrin in common organic solvents forms an inclusion complex with C_{60} (Chart 1).[7] The complex is much more stable than previous examples,[2] and does not dissociate even under chromatographic conditions. Later, we also found that a proper choice of linker parts for the cyclic dimer is quite important for the high affinity toward fullerenes. Furthermore, the binding capability of the host molecule is widely tunable using the central metal ions of the porphyrin moieties. Together with the design flexibility of the porphyrin skeleton, one may readily prepare a library of host molecules for different purposes. This is one of the great advantages of the metalloporphyrin-based cyclic host molecules.

Cyclic metalloporphyrin hosts

General features of complexation with fullerenes

The zinc porphyrin cyclic dimer **10** (Table 1) forms a highly stable 1 : 1 inclusion complex with C_{60} ($\mathbf{10} \supset C_{60}$), where the association constant (K_{assoc}) in benzene at 25 °C (6.7×10^5 M^{-1}) is more than an order of magnitude greater than those with other types of host molecules so far reported.[7] Due to such a high affinity of the host molecule toward fullerenes, inclusion complex $\mathbf{10} \supset C_{60}$ is isolable by chromatography, and its molecular ion peak can be detected using electrospray ionization mass spectrometry. Interestingly, cyclic dimer **12**, a synthetic precursor of **10**, which has rigid diacetylenic linkers between the two metalloporphyrin moieties (Table 1), does not show any sign of complexation with fullerenes. This observation indicates the importance of a certain conformational flexibility in the linker parts of the host molecule, most likely for adjusting the porphyrin–porphyrin distance to maximize the interaction. Fig. 1 shows the X-ray crystallographic structure of an inclusion complex between **11** (Table 1) and C_{60} ($\mathbf{11} \supset C_{60}$), where guest C_{60} is located at the centre of the π-electronic host cavity.[8] One may also recognize that the zinc porphyrin moieties adopt a nonplanar, concave structure. Furthermore, the C6 alkylene linkers of the host are folded to achieve a better contact with C_{60}. Judging from the complexity of the ^1H and ^{13}C NMR spectral features, the cyclic hosts without fullerene guests exist as a mixture of some conformational isomers in solution. However, upon addition of, *e.g.*, C_{60}, these NMR spectra are substantially simplified, indicating that the inclusion complexation is accompanied by an induced-fit conformational change in the host molecules. The inclusion event can also be visualized by a bathochromic absorption spectral change in the host molecules. Upon inclusion of C_{60}, for instance, host **10** shows a red shift of the Soret absorption band of the metalloporphyrin moiety with a decrease in intensity (Fig. 2). At the same time, it displays a broad absorption band at 750–850 nm, assignable to

Table 1 Molecular structures and formulae of metalloporphyrin hosts **1–13**

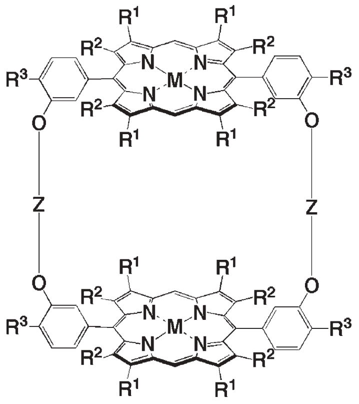

Host	Z	R^1	R^2	R^3	M
1	$-(CH_2)_4-$	H	H	$OC_{12}H_{25}$	CH_3Rh(III)
2	$-(CH_2)_5-$	H	H	$OC_{12}H_{25}$	Zn(II)
3	$-(CH_2)_6-$	H	H	$OC_{12}H_{25}$	Zn(II)
4	$-(CH_2)_6-$	C_6H_{13}	CH_3	H	2H
5	$-(CH_2)_6-$	C_6H_{13}	CH_3	H	Co(II)
6	$-(CH_2)_6-$	C_6H_{13}	CH_3	H	CH_3Rh(III)
7	$-(CH_2)_6-$	C_6H_{13}	CH_3	H	Ni(II)
8	$-(CH_2)_6-$	C_6H_{13}	CH_3	H	Cu(II)
9	$-(CH_2)_6-$	C_6H_{13}	CH_3	H	Ag(II)
10	$-(CH_2)_6-$	C_6H_{13}	CH_3	H	Zn(II)
11	$-(CH_2)_6-$	C_2H_5	C_2H_5	H	Zn(II)
12	$-CH_2C\equiv C-C\equiv CCH_2-$	C_6H_{13}	CH_3	H	Zn(II)
13	$-(CH_2)_7-$	H	H	$OC_{12}H_{25}$	Zn(II)

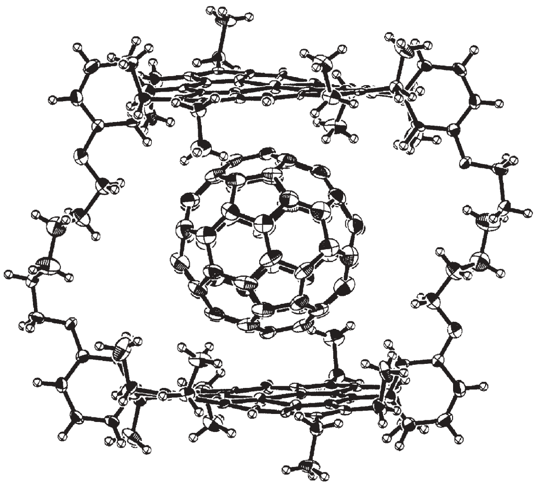

Fig. 1 ORTEP diagram of an inclusion complex of C_{60} with **11** ($\mathbf{11} \supset C_{60}$).

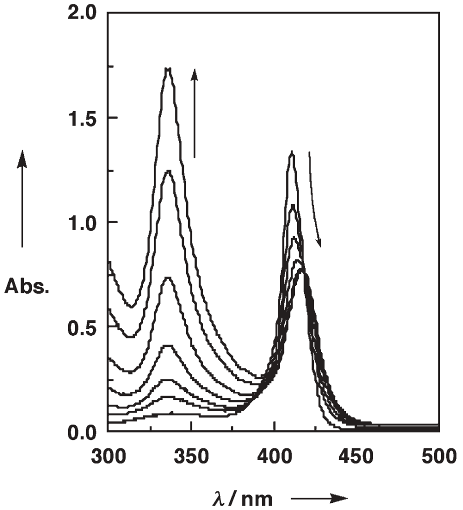

Fig. 2 Spectroscopic titration of host **10** with C_{60} in benzene at 25 °C. [**10**] = 2.0×10^{-6} M; [C_{60}]/[**10**] = 0–15.

a zinc porphyrin-to-fullerene charge-transfer interaction.[9] In harmony with this observation, the first reduction potential of included C_{60} (-1.11 V *vs.* Fc/Fc^+ in CH_2Cl_2 at 25 °C) is more negative than that of uncomplexed C_{60} (-1.05 V). ^{13}C NMR spectroscopy of the inclusion complex of **10** with C_{60} in C_6D_6 at 30 °C shows a single signal due to included C_{60} at δ 140.1 ppm, which is upfield-shifted from that of free C_{60} (δ 143.2). Such an upfield shift most likely reflects an electronic effect of the zinc porphyrin π-cloud on the fullerene guest.

Porphyrin dimers, if acyclic, show a very low affinity toward fullerenes.[10] However, when the two metalloporphyrin moieties are allowed to adopt a cyclic geometry *via*, *e.g.*, intramolecular hydrogen-bonding interactions, fullerenes are included into the resulting cavity, where the K_{assoc} value is just an order of magnitude smaller than those of its covalent analogues.[11] Metal coordination appears to be more promising than hydrogen-bonding to realize a cyclic structure in the non-covalent design of host molecules. An example is shown by the Pd(II)-directed dimerization of a pyridylporphyrin, where the porphyrin moieties of the resulting dimer, though acyclic, sandwich C_{60} with a K_{assoc} value of 5.2×10^3 M^{-1} in toluene-d_8 at room temperature.[12]

Structure–affinity relationships

Cyclodimeric metalloporphyrin hosts tend to prefer larger fullerenes due to a better contact between their π-electronic surfaces.[8,13] When host **10** (Table 1) is used, the observed K_{assoc} value with C_{70} (Chart 1) is 30 times larger than that with C_{60}.[8] Similar to the case of C_{60}, the ^{13}C NMR signals due to C_{70} in the inclusion complex are upfield-shifted from those of uncomplexed C_{70}. Since such an upfield shift is more pronounced for the equatorial carbon signals than for those located at the poles, C_{70} appears to adopt a side-on conformation with respect to the two metalloporphyrin moieties in order to maximize the host–guest π-electronic interactions. When compound **3**, a pyrrole-β-unsubstituted analogue of **10**, is used as the host molecule, the affinity toward fullerenes is lower, partially due to the lower π-basicity of its porphyrin moieties, resulting in a smaller extent of the porphyrin-to-fullerene charge-transfer.[13] In addition to this, pyrrole-β-unsubstituted porphyrins prefer to adopt a planar conformation due to the absence of steric repulsions at their periphery. This is in contrast with porphyrins that have pyrrole-β-substituents such as those in host **11**, which bear a steric repulsion between the *meso*-aryl groups and the neighbouring pyrrole-β-substituents. The resulting concave conformation of the zinc porphyrin units in **11** appears to be important for the better host–guest contact (Fig. 1).

Not only the structures of the porphyrin and linker parts but also the central metal ions of the porphyrin moieties significantly affect the binding capability of the host molecule toward fullerenes. As shown in Fig. 3a, the affinity of zinc porphyrin host **10** toward C_{60} is comparable to that of free-base host **4**, while host molecules **7–9** with Ni(II), Cu(II) and Ag(II), respectively (Table 1), are inferior to the above two hosts.[8] On the other hand, hosts **5** and **6** bearing Group 9 metal ions such as Co(II) and Rh(III), respectively (Table 1), display a much larger affinity toward fullerenes. In particular, the K_{assoc} value of Rh(III)-containing host **6** with C_{60} is quite large; in benzene at 25 °C it is 2.4×10^7 M^{-1}.[8] A similar metal ion-dependence has been observed for the complexation with C_{70} (Fig. 3b), where an extremely large K_{assoc} value ($\sim 10^8$ M^{-1}), observed for the complexation of **6** with C_{70}, is noteworthy as it is nearly comparable to that of a quadruple hydrogen-bonding interaction.[14] Rh(III) species are known to add to double bonds. Likewise, a certain Rh(III) porphyrin has

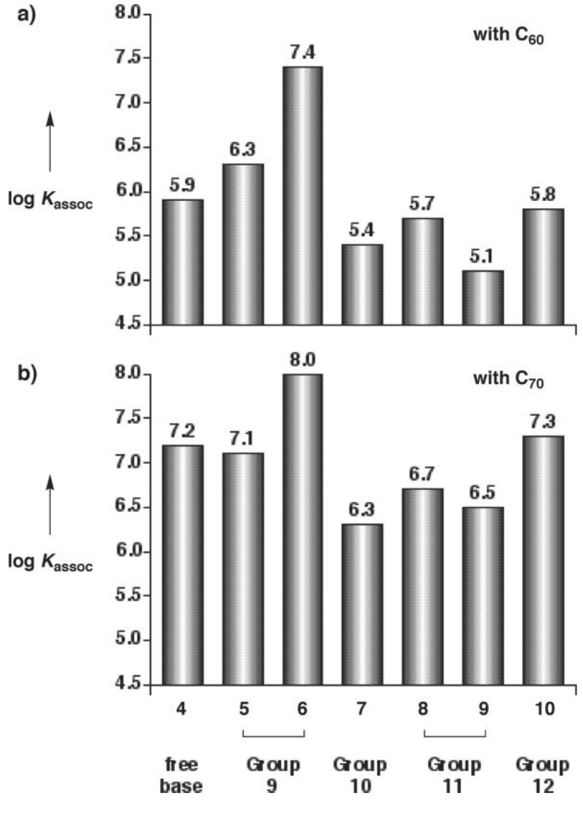

Fig. 3 Association constants K_{assoc} of metalloporphyrin hosts **4–10**, which have different metal ions, with (a) C_{60} and (b) C_{70} in benzene at 25 °C.

been reported to form an ethene π-complex.[15] Quite interestingly, we have found that C_{70}, which, in the cavity of **6**, adopts a side-on orientation with respect to the porphyrin moieties, turns to an end-on orientation upon lowering the temperature from 25 °C down to −60 °C. It is likely that the side-on orientation is a thermodynamically favoured conformation, as it allows a better π-electronic host–guest contact. On the other hand, the end-on orientation of C_{70} allows the Rh(III) ions of the host molecule to interact directly with the π-electron-rich 6:6 ring junctions close to the pole.[16] This observation clearly indicates the positive contributions of the central Rh(III) ions of the porphyrin moieties to the binding of fullerenes. In agreement with this observation, when the axial group attached to each Rh(III) ion is changed from the methyl group to the electron-withdrawing acetyl group, the K_{assoc} value of the host becomes nearly an order of magnitude smaller.

All the host molecules described above possess C6 alkylene chains to connect the porphyrin units. According to ^{1}H NMR spectroscopy, the two metalloporphyrin units in the hosts, upon inclusion of fullerenes, adopt on average a parallel orientation to one another. While the same is true for the inclusion complexes that have C5 and C7 alkylene linkers,[13] those having C4 linkers behave differently from the other hosts.[17] The porphyrin–porphyrin distance (at most 11.8 Å; CPK model) of C4 alkylene-linked host **1** (Table 1), for example, is not large enough to accommodate fullerenes in a similar manner to the above hosts bearing longer alkylene linkers. When the central metal ions of the porphyrin units are Rh(III), such a small host still shows an adequate binding affinity toward fullerenes, while the association constants, however, are an order of magnitude smaller than those with longer-spaced host molecules. Quite interestingly, ^{1}H NMR spectroscopy shows that the metalloporphyrin units in $\mathbf{1}\supset\mathrm{C}_{60}$ adopt a tilted geometry to accommodate C_{60} (Fig. 4a). Furthermore, in the presence of a large excess of **1** with respect to C_{60}, capsule-type 2 : 1 host–guest complex $\mathbf{1}_2\supset\mathrm{C}_{60}$ concomitantly forms (Fig. 4b), where the K_{assoc} value of the second-bound **1** is two orders of magnitude smaller than that of the first-bound **1**. Since the steric repulsion between the two molecules of **1** incorporated in $\mathbf{1}_2\supset\mathrm{C}_{60}$ is negligible, such a large difference in the K_{assoc} value between the first and second host-binding events is most likely due to a negative electronic effect of the first-bound **1** on the second host-binding.

Dynamic aspects

In order to obtain the crystal structure of inclusion complex $\mathbf{11}\supset\mathrm{C}_{60}$ (Fig. 1), lowering the temperature to, *e.g.*, −110 °C is essential. Otherwise, only the host structure can be crystallographically determined, indicating a possible thermal rotation of guest C_{60} in the host cavity. In solution, guest C_{60} must undergo much more complicated motions. For example, in toluene-d_8 at 40 °C, guest C_{60} included in **10** exchanges with uncomplexed C_{60} very frequently.[8] ^{13}C NMR spectroscopy of a mixture of C_{60} and **10** at a 2 : 1 molar ratio shows only a single signal at δ 141.6 ppm. On the other hand, upon lowering the temperature to −60 °C, the single signal splits into two signals at δ 139.7 and 142.9 ppm, which are assignable to complexed and uncomplexed C_{60}, respectively. Variable-temperature ^{13}C NMR spectroscopy (Fig. 5a) shows that these signals start to coalesce at 20 °C, where the guest exchange occurs at a rate of 450 times per second.[8] Use of C_{70} as the guest results in a similar temperature-dependent spectral change profile, where the observed coalescence temperature (60 °C), however, is higher than the case with C_{60}, possibly due to the larger affinity of C_{70} toward host **10**. In sharp contrast, although the K_{assoc} value for the inclusion of Rh(III)-containing host **6** with C_{60} ($\mathbf{6}\supset\mathrm{C}_{60}$) is as large as that for $\mathbf{10}\supset\mathrm{C}_{70}$, a 1 : 2 mixture of **6** and C_{60} displays two well split signals due to complexed and uncomplexed C_{60} over a wide temperature range, even at 100 °C (Fig. 5b). Considering the fact that the K_{assoc} values (= $k_{\mathrm{assoc}}/k_{\mathrm{dissoc}}$) for $\mathbf{10}\supset\mathrm{C}_{70}$ and $\mathbf{6}\supset\mathrm{C}_{60}$ are both large and in the range of 10^7 M^{-1}, the guest exchange dynamics are mainly determined by the rate constant for guest dissociation. Thus, the obviously slower guest exchange dynamics of $\mathbf{6}\supset\mathrm{C}_{60}$ compared to $\mathbf{10}\supset\mathrm{C}_{70}$ demonstrates that host **6** releases the fullerene guest much more slowly than **10**. This result again indicates the special interactions of the Rh(III) ions of **6** with included fullerenes.

By using dumbbell-shaped C_{120}[18] (Chart 1) as the guest, we found another interesting dynamic motion, *i.e.*, oscillation (Scheme 1).[19] Mixing of C_{120} with **6** at a 1 : 1 molar ratio in

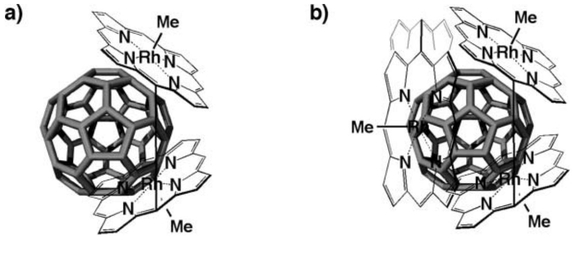

Fig. 4 Structures of (a) 1 : 1 and (b) 2 : 1 host–guest complexes composed of host **1** and C_{60}.

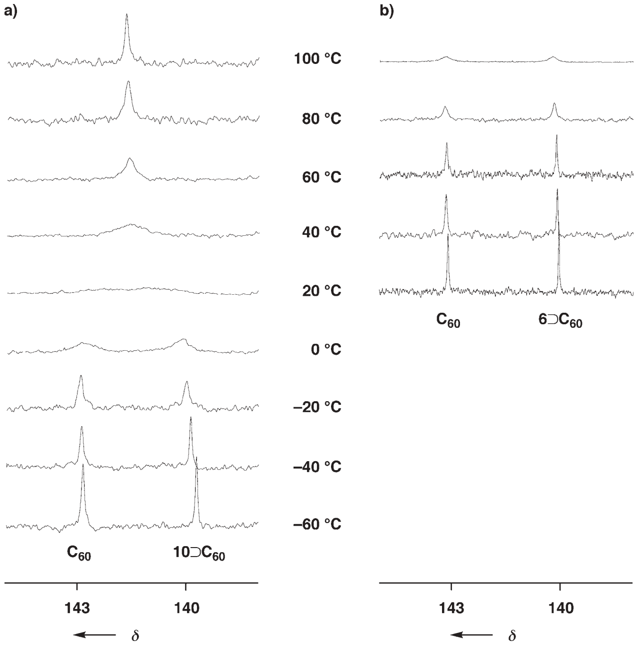

Fig. 5 Variable-temperature ^{13}C NMR profiles of ^{13}C-enriched C_{60} in the presence of 0.5 equiv. of (a) **10** and (b) **6** in toluene-d_8.

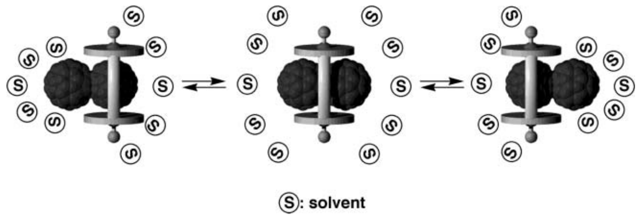

Scheme 1 Schematic representation of an oscillatory motion of C_{120} in the cavity of **6** coupled with its desolvation/solvation dynamics.

toluene results in selective formation of a pseudo rotaxane-type 1 : 1 inclusion complex $\mathbf{6}\supset C_{120}$, while $\mathbf{6}_2\supset C_{120}$ concomitantly forms in the presence of an excess amount of **6** with respect to C_{120}. Inclusion complex $\mathbf{6}\supset C_{120}$ shows two ^{1}H NMR signals for both the *meso* and pyrrole-β-methyl protons, due to the protrusion of one of the C_{60} moieties of C_{120}. However, upon elevation of the temperature, these signals coalesce to give a single set of signals for the corresponding protons. Although such a spectral coalescence is possibly induced by guest exchange as well as guest oscillation, a separate experiment indicates that the guest exchange is noticeably slower than the oscillatory motion of C_{120}. From line shape analysis of variable-temperature ^{1}H NMR spectral profiles of $\mathbf{6}\supset C_{120}$, guest C_{120} has been evaluated to oscillate at ~1200 times per second at 70 °C.[19] Interestingly, the oscillation frequency shows a marked solvent dependency, where better solvents for fullerenes give rise to lower oscillation frequencies. This trend is totally opposite to our initial expectation that the host molecules in better solvents for fullerenes must loosely capture C_{120} as the K_{assoc} values are smaller, and therefore allow a more rapid oscillation of C_{120}. Later, we noticed that the oscillatory motion of included C_{120} mostly reflects the desolvation/solvation dynamics of the protruding C_{60} moiety of C_{120} from the host cavity (Scheme 1). The $\Delta S^{\ddagger}$ value for the oscillation is always positive irrespective of the solvent polarity, suggesting that the oscillation is driven entropically and occurs through a less solvated transition state.

When a host molecule with shorter linkers such as **1** is used, even fullerene monomers C_{60} and C_{70} display an oscillatory motion (Scheme 2).[17] As already described, the two metalloporphyrin units in guest-binding **1** adopt a tilted geometry with respect to one another (Fig. 4a). According to variable-temperature NMR spectral profiles, guest C_{60} undergoes a much faster slip-through motion (335 s^{-1} at −80 °C) than C_{70} (40 s^{-1} at −60 °C) in the cavity of **1**. On the other hand, C_{76}[20] (Chart 1) is too large to get through the cavity of **1** and hardly oscillates. As expected, in the presence of an excess amount of **1** with respect to C_{60}, such an oscillatory motion is totally disabled due to the formation of capsule-type $\mathbf{1}_2\supset C_{60}$. Thus, host **1** may be called a self-regulating host, where capping of the 1 : 1 host–guest complex by the second host molecule substantially prohibits the slip-through guest motion (Scheme 2).

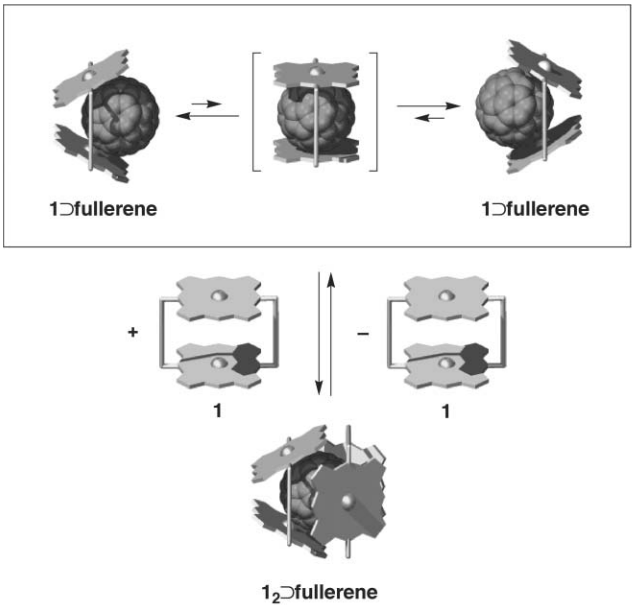

Scheme 2 Schematic representations of the complexation behaviour of **1** with fullerenes and accompanying dynamic events.

Cyclic hosts with π-extended metalloporphyrins

Cyclic hosts composed of fused metalloporphyrin oligomers are quite interesting, as they might accommodate a larger number of fullerene guests than those consisting of metalloporphyrin monomers. In this context, we have synthesized a novel cyclic host that bears two fused zinc porphyrin dimers (**14**; Chart 2).[21] As expected, host **14** is able to form a highly stable inclusion complex with C_{120}. On the other hand, when C_{60} is the guest, one can see a unique binding feature of **14** originating from a π-electronic conjugation between the two zinc porphyrin units in their fused array. Namely, host **14** displays a negative homotropic cooperative binding for both C_{60} and diamines, while it shows a positive heterotropic cooperative binding for a mixture of C_{60} and diamines.[21,22]

For example, while host **14** in toluene at 20 °C can accommodate two molecules of 4,4′-bipyridine (bpy), the K_{assoc} value for the second bpy is 12 times smaller than that for the first bpy.[21] Obviously, bpy is an electron-donating guest. Therefore, the negative cooperativity observed for the binding of bpy can be explained by the fact that electron donation from the first-bound bpy is transmitted through a π-electronic conjugation over the fused porphyrin array to the other binding site and hampers the complexation of the second bpy.

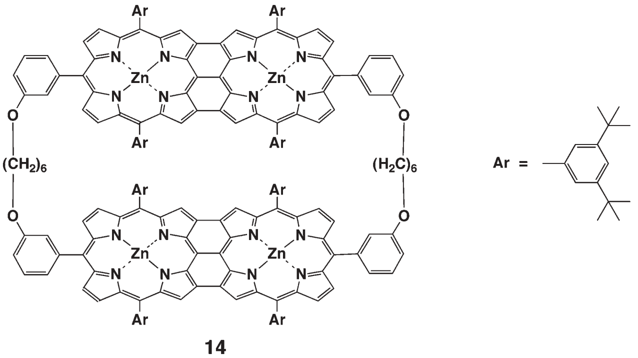

14

Chart 2 Schematic molecular structure of host **14** composed of two fused zinc porphyrin dimer units.

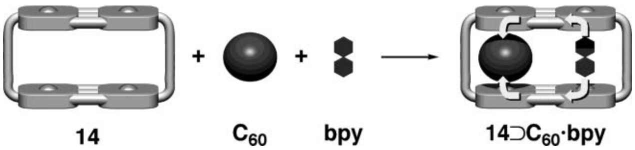

Scheme 3 Schematic representation of the selective formation of hetero-guest pair C_{60}·bpy upon mixing C_{60} and 4,4′-bipyridine (bpy) with host **14**.

In contrast to bpy, with zinc porphyrins C_{60} behaves like an electron-accepting guest. Quite interestingly, the feature of negative homotropic cooperative binding, observed for bpy, is even more explicit for C_{60}.[22] Although host **14** possesses such a large cavity that it can accommodate C_{120}, it can trap only one molecule of C_{60}. Here, we assume that inclusion of C_{60} into the cavity of **14** may entirely reduce the electron-donating capability of the fused zinc porphyrin array, thereby disfavouring the binding of the second C_{60}.

Since the electronic effects of bpy and C_{60} toward the metalloporphyrin moieties of the host are opposite to one another, host **14** might accommodate both bpy and C_{60} simultaneously in its cavity. This is actually true.[22] Inclusion of bpy results in enhancing the affinity of the host toward C_{60} by a factor of 8.5 (positive heterotropic cooperativity). On the other hand, the C_{60}-containing **14** is 6.1 times more active than the guest-free host for the complexation with a base such as *N*,*N*,*N*′,*N*′-tetramethylhexane-1,6-diamine. In these cases, the electronic effect of the first-bound guest is always favourable for the second guest, since the electronic effects of these guests are complementary to one another (Scheme 3). The positive heterotropic cooperative binding, thus realized electronically, is quite interesting, since all precedent examples for the formation of hetero-guest pairs have made use of van der Waals fitting as the common strategy.[23]

In addition to such electronic effects, guest-induced conformational motions of hosting molecules have been shown to be usable for the cooperative binding of fullerenes. An example is given by the use of a rigid dendritic molecule with multiple zinc porphyrin units, where binding of a fullerene guest results in a conformational change in the dendritic scaffold to form the next binding site.[24]

Discrimination of fullerenes

All the above observations have prompted us to explore the possibility of discriminating fullerenes in terms of their dimensions and chirality.

Selective extraction of rare fullerenes

Fullerenes $\geqslant C_{76}$ are called 'higher fullerenes',[25] and have attracted attention as they allow studies on structure–property relationships of discrete π-conjugated nanocarbons. However, a practical difficulty in isolating such low-yield combustion products has prevented exploration of their physical properties as well as their applications to materials sciences.

While pyrrole-β-substituted host **10**, often used in our study, does not behave well in the selective extraction of higher fullerenes, host **3**, without pyrrole-β-substituents, is much better.[13] In addition to **3**, pyrrole-β-unsubstituted hosts with shorter and longer linkers, such as **2** and **13** (Table 1), respectively, have been investigated as references. Typically, host **3** is added to a toluene solution of a fullerene mixture, obtained from a combustion-based industrial production source, and THF is added to the resulting solution to allow precipitation of uncomplexed fullerenes. The filtrate is evaporated to dryness, and the residue is chromatographed on alumina, where a fraction containing the zinc porphyrin host is isolated and treated with bpy to allow dissociation of included fullerenes from the host cavity. The reaction mixture is subjected to size-exclusion chromatography to isolate a fraction containing fullerenes, which is washed with aqueous AcOH to remove bpy. For analysis, the extract is subjected to analytical HPLC on a 5-PBB column with chlorobenzene as an eluent.

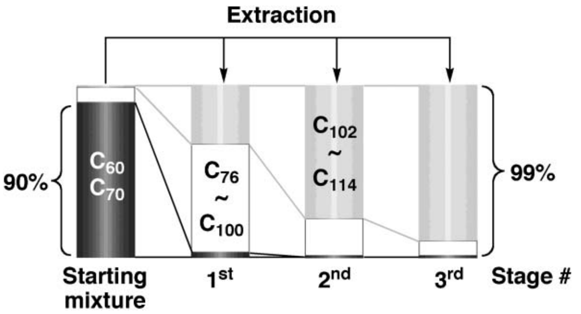

Fig. 6 Abundances (abs%) of C_{60}–C_{70} (black bars), C_{76}–C_{100} (white bars) and C_{102}–C_{114} (grey bars) in a starting fullerene mixture and fractions obtained after the first, second and third-stage extractions with host **3**.

Single extraction of the fullerene mixture with **3** allows enrichment of fullerenes $\geqslant C_{76}$, with their overall content up to 93% (Fig. 6) from that in the starting mixture (10%), where the enrichment of C_{96} is most remarkable (0.4% [Fig. 7a] → 36% [Fig. 7b]). Two more repetitions of this extraction afford a fraction containing very rare fullerenes such as C_{102}–C_{110} (initial abundance <0.1%) up to 82% (Fig. 7d). While extraction with host **2** does not give satisfactory results, host **13** furnishes a 97% overall content of fullerenes $\geqslant C_{76}$.

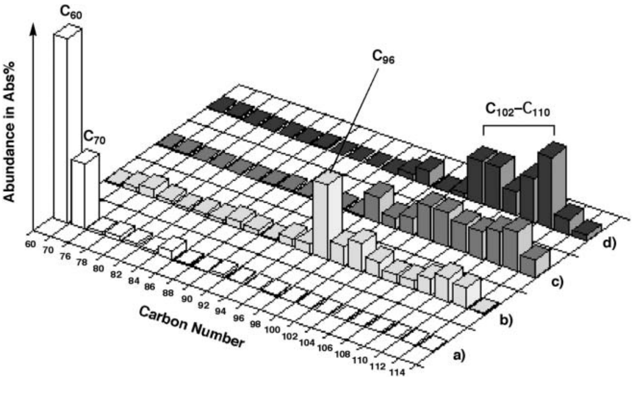

Fig. 7 Abundances (abs%) of C_{60}–C_{114} in (a) a starting fullerene mixture and fractions after (b) the first, (c) second and (d) third-stage extractions with host **3**.

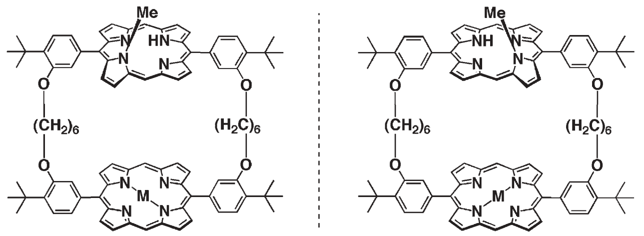

(±)-15: M = CH$_3$Rh
(±)-16: M = 2H

Chart 3 Schematic molecular structures of the enantiomers of chiral metalloporphyrin hosts **15** and **16**.

Chiral discrimination

Some higher fullerenes such as C_{76}, C_{78} and C_{84} are chiral.[26] In relation to the discrimination of metallic and semiconducting carbon nanotubes, design of host molecules for recognizing chiral fullerenes is one of the most challenging issues.[27] Since chiral fullerenes are devoid of any appropriate functionalities for point recognition, their chirality sensing certainly requires a different strategy from those for ordinary asymmetric compounds.

Very recently, we have found that host **15** (Chart 3), which bears a chiral *N*-methyldiarylporphyrin ($\mathbf{P_{NMe}}$) moiety, with the symmetry group C_1, on the other side of a methylrhodium diarylporphyrin ($\mathbf{P_{Rh}}$) unit, can spectroscopically discriminate enantiomers of C_{76}.[28] When a racemic mixture of C_{76} (($\pm$)-C_{76}) in toluene-d_8 is allowed to complex with ($\pm$)-**15** at 20 °C, the NH proton of $\mathbf{P_{NMe}}$ shows two split signals at δ −2.76 and −2.79 ppm, assignable to diastereoisomers (−)-**15**$\supset$(+)-C_{76}/(+)-**15**$\supset$(−)-C_{76} and (+)-**15**$\supset$(+)-C_{76}/(−)-**15**$\supset$(−)-C_{76}, respectively. Here, the $\mathbf{P_{Rh}}$ unit as well as the chiral $\mathbf{P_{NMe}}$ moiety of **15** appear to contribute to the chiral discrimination of C_{76}, since metal-free reference **16** hardly displays diastereoisomerically split ^{1}H NMR signals upon complexation with ($\pm$)-C_{76}. The difficulty in chiral discrimination with **16** is due to the rather low affinity of **16** toward fullerenes, allowing a faster guest exchange than the ^{1}H NMR timescale.

Thanks to a good resolution in the diastereoisomerically split NH signals (15.6 Hz) of **15**$\supset C_{76}$ (Fig. 8a), accurate determination of the enantiomeric purity of C_{76} is possible. Plots of the enantiomeric purity of guest C_{76}, as determined by the integral ratios of the NH signals of $\mathbf{P_{NMe}}$ in (−)-**15**$\supset C_{76}$, *versus* the $\Delta\varepsilon$ values of C_{76} give a linear correlation. Extrapolation of the fitted line of the plots to the enantiomeric purity of 100% (Fig. 8b) provides an absolute $\Delta\varepsilon$ value of 58.5 M^{-1} cm^{-1} for enantiomerically pure C_{76} in toluene at 330 nm. This value is larger than those obtained so far *via* direct chiral HPLC separation (14.3 M^{-1} cm^{-1})[29] or methods involving chemical transformations (53.4 M^{-1} cm^{-1}).[30]

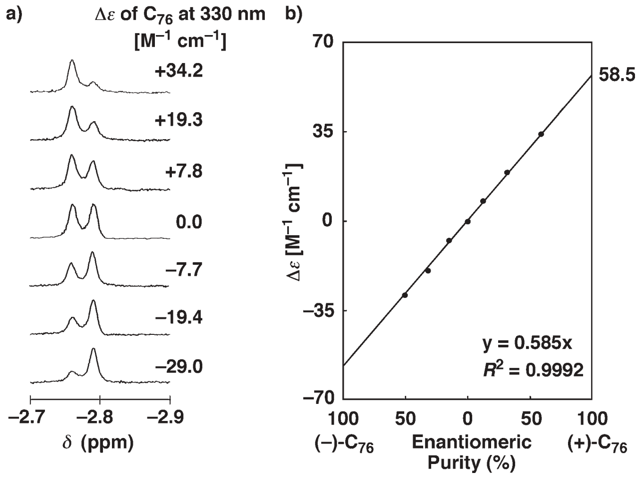

Fig. 8 (a) ^{1}H NMR (500 MHz) spectra (NH signals of $\mathbf{P_{NMe}}$) of equimolar mixtures of (−)-**15** and C_{76} of different $\Delta\varepsilon$ values ([C_{76}] = 1.5 × 10^{-4} M) in toluene-d_8 at 20 °C. (b) Plots of the enantiomeric purity of C_{76}, as determined by the integral ratios of the NH signals of (−)-**15**$\supset C_{76}$, *versus* $\Delta\varepsilon$ values of C_{76} in toluene at 20 °C.

Hybridization and controlled self-assembly

Polymer composites of fullerenes

Hybridization of fullerenes with polymers is a practically important subject for possible fabrication of electro- and optoelectroactive plastic materials.[31] However, the poor compatibility of fullerenes with commodity polymers sometimes becomes an essential issue. While covalent functionalization of fullerenes with proper organic groups miscible with commodity polymers is certainly a promising strategy to overcome this problem,[32] it inevitably results in partial destruction of the π-electronic conjugation of fullerenes.

We have synthesized poly(benzyl ether) dendrimer **17** that has at its centre a cyclic dimer of porphyrin (Chart 4).[33] This dendritic host can incorporate fullerenes into the cavity of its core unit and solubilize them in a variety of solvents, depending on the solubility of the dendritic wedges. Furthermore, thanks to the high compatibility of poly(benzyl ether) dendrimers with commodity polymers, dendritic host **17** allows a highly stable, molecular-level dispersion of fullerenes in, *e.g.*, poly(methyl methacrylate), affording a homogeneous composite film.[33] In the absence of host **17**, C_{60} formed conglomerates in such a polymeric matrix.

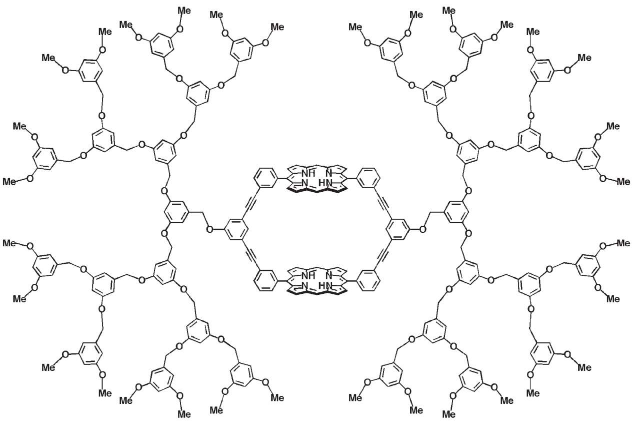

17

Chart 4 Schematic molecular structure of host **17** with poly(benzyl ether) dendritic wedges.

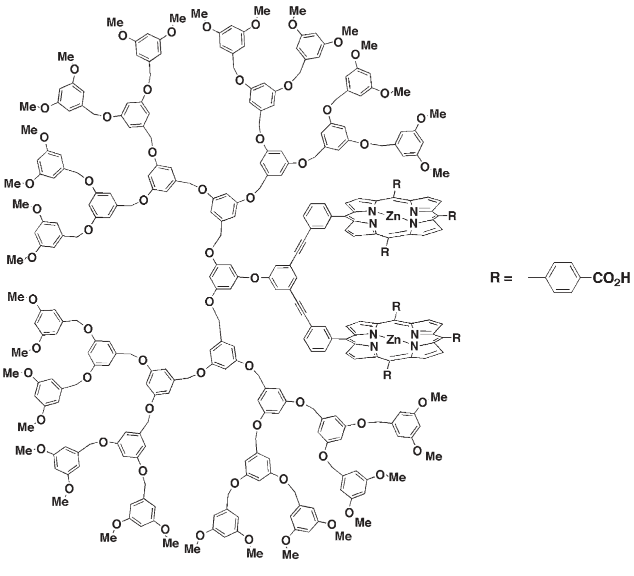

18

Chart 5 Schematic molecular structure of dendrimer-appended host **18** that has carboxylic acid functionalities for self-assembly.

Supramolecular peapods

Compound **18** (Chart 5) is another type of dendritic host, bearing at its focal core an acyclic dimer of a zinc porphyrin.[34] We happened to notice that this dendritic molecule co-assembles with fullerenes such as C_{60} and C_{70} to form an interesting low-dimensional nanostructure referred to as a 'supramolecular peapod', where included fullerenes are aligned within a dendrimer-coated supramolecular porphyrin nanotube. Peapod-like fullerene-included carbon nanotubes (Fig. 9) have attracted attention due to their unique electronic properties that arise from hybridization of carbon nanotube π-electrons with those of the inner fullerenes.[35]

The zinc porphyrin dimer, at the focal core of compound **18**, is acyclic and may not be suitable for the incorporation of fullerenes. However, because of the presence of carboxylic acid groups, this acyclic core, upon interaction with fullerenes, undergoes a guest-directed cyclodimerization *via* intermolecular hydrogen-bonding interactions (Scheme 4). The fullerene-included supramolecular dimer, thus formed, is further assembled bilaterally *via* hydrogen-bonding interactions of the residual carboxylic acid groups, to accomplish the peapod structure (Scheme 4). According to TEM analysis (Fig. 10a), the resulting low-dimensional nanostructure is several micrometres long and possesses a uniform diameter of 15 nm, in agreement with a prediction from the CPK model (12 nm). Without fullerenes, compound **18** only forms an irregular hydrogen-bonded aggregate (Fig. 10b) due to conformational freedom in the acyclic core. At −40 °C, included C_{60} within the porphyrin nanotube shows a broad ^{13}C NMR signal at δ 139.6 ppm in 1,1,2,2-tetrachloroethane-d_2, indicating highly constrained motion of C_{60} in the tubular space.

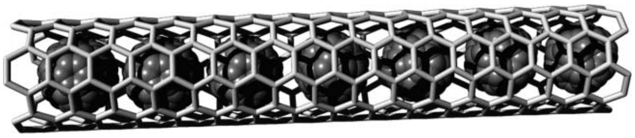

Fig. 9 Schematic representation of a C_{60}-included carbon nanotube.

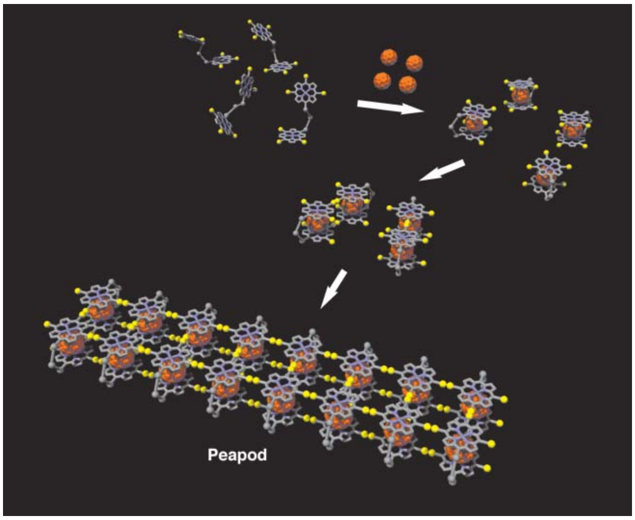

Scheme 4 Schematic representation of one-dimensional supramolecular polymerization of CO_2H (yellow)-appended acyclic zinc porphyrin dimer **18** directed by a π-electronic interaction with fullerenes.

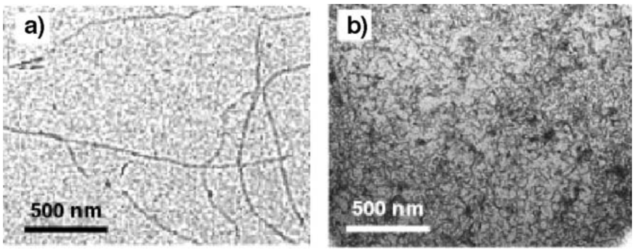

Fig. 10 TEM micrographs of (a) **18** with C_{60} and (b) **18** alone. Samples were cast from 1,1,2,2-tetrachloroethane after heating once at 120 °C, followed by incubation at 40 °C for 4 days, and staining with RuO_4.

Conclusions

Despite the great potential of metalloporphyrins as hosting molecules for fullerenes, host–guest chemistry in solution involving these two π-electronic molecules had been unprecedented until rather recently, since metalloporphyrin monomers, contrary to the above expectation, hardly interact with fullerenes in solution. In fact, our cyclodimeric zinc porphyrin host **10**, which led to the discovery of the novel inclusion chemistry of fullerenes, was designed for a different purpose. Through our extensive studies, which date back to 1998, along with those by other research groups, the host–guest chemistry of fullerenes with engineered metalloporphyrin hosts has progressed a lot. It is now an important aspect of supramolecular chemistry, not only covering fundamental aspects but also some unique applications, such as visualization of restricted motions of fullerenes, including their desolvation/solvation dynamics, cooperative host–guest complexation phenomena due to long-range electronic communication through π-conjugation and discrimination of the dimensions and chirality of fullerenes. Furthermore, programmed self-organization to construct low-dimensional nanostructures of fullerenes could contribute to the fabrication of functional nanomaterials for electronic and optoelectronic applications.

Acknowledgements

We thank Profs K. Saigo, K. Kinbara, J.-Y. Zheng, K. Yamaguchi, K. Komatsu, A. Osuka and T. Akasaka, together with Drs S. Sakamoto, Y. Murata, N. Ishii, H. Shinmori and T. Tsuchiya for their active collaborations. K. T. thanks the Industrial Technology Research Grant Program in '04 from the New Energy and Industrial Technology Development Organization (NEDO) of Japan for financial support.

References

1 F. Diederich and M. Gómez-López, *Chem. Soc. Rev.*, 1999, **28**, 263 and references therein.
2 T. Haino, M. Yanase and Y. Fukazawa, *Angew. Chem., Int. Ed.*, 1998, **37**, 997 and references therein.
3 R. S. Ruoff, D. S. Tse, R. Malhotra and D. C. Lorents, *J. Phys. Chem.*, 1993, **97**, 3379.
4 *The Porphyrin Handbook*, ed. K. M. Kadish, K. M. Smith and R. Guilard, Academic Press Inc., San Diego, 1999.
5 P. D. W. Boyd and C. A. Reed, *Acc. Chem. Res.*, 2005, **38**, 235 and references therein.
6 H. Imahori and Y. Sakata, *Eur. J. Org. Chem.*, 1999, 2445 and references therein.
7 K. Tashiro, T. Aida, J.-Y. Zheng, K. Kinbara, K. Saigo, S. Sakamoto and K. Yamaguchi, *J. Am. Chem. Soc.*, 1999, **121**, 9477.
8 J.-Y. Zheng, K. Tashiro, Y. Hirabayashi, K. Kinbara, K. Saigo, T. Aida, S. Sakamoto and K. Yamaguchi, *Angew. Chem., Int. Ed.*, 2001, **40**, 1857.
9 K. Tashiro and T. Aida, *J. Inclusion Phenom. Macrocyclic Chem.*, 2001, **41**, 215.
10 D. Sun, F. S. Tham, C. A. Reed, L. Chaker and P. D. W. Boyd, *J. Am. Chem. Soc.*, 2002, **124**, 6604.
11 Z.-Q. Wu, X.-B. Shao, C. Li, J.-L. Hou, K. Wang, X.-K. Jiang and Z.-T. Li, *J. Am. Chem. Soc.*, 2005, **127**, 17460.
12 D. Sun, F. S. Tham, C. A. Reed, L. Chaker, M. Burgess and P. D. W. Boyd, *J. Am. Chem. Soc.*, 2000, **122**, 10704.
13 Y. Shoji, K. Tashiro and T. Aida, *J. Am. Chem. Soc.*, 2004, **126**, 6570.
14 R. P. Sijbesma, F. H. Beijer, L. Brunsveld, B. J. B. Folmer, J. H. K. K. Hirschberg, R. F. M. Lange, J. K. L. Lowe and E. M. Meijer, *Science*, 1997, **278**, 1601.
15 B. B. Wayland, S. L. Van Voorhees and K. J. Del Rossi, *J. Am. Chem. Soc.*, 1987, **109**, 6513.
16 R. Taylor, *J. Chem. Soc., Perkin Trans. 2*, 1993, 813.
17 A. Ouchi, K. Tashiro, K. Yamaguchi, T. Tsuchiya, T. Akasaka and T. Aida, *Angew. Chem., Int. Ed.*, 2006, **45**, 3542.
18 G.-W. Wang, K. Komatsu, Y. Murata and M. Shiro, *Nature*, 1997, **387**, 583.
19 K. Tashiro, Y. Hirabayashi, T. Aida, K. Saigo, S. Sakamoto, K. Yamaguchi, K. Fujiwara and K. Komatsu, *J. Am. Chem. Soc.*, 2002, **124**, 12086.
20 R. Ettl, I. Chao, F. Diederich and R. L. Whetten, *Nature*, 1991, **353**, 149.
21 H. Sato, K. Tashiro, H. Shinmori, A. Osuka and T. Aida, *Chem. Commun.*, 2005, 2324.
22 H. Sato, K. Tashiro, H. Shinmori, A. Osuka, Y. Murata, K. Komatsu and T. Aida, *J. Am. Chem. Soc.*, 2005, **127**, 13086.
23 M. Yoshizawa, T. Takeyama, T. Okano and M. Fujita, *J. Am. Chem. Soc.*, 2003, **125**, 3243 and references therein.
24 M. Ayabe, A. Ikeda, Y. Kubo, M. Takeuchi and S. Shinkai, *Angew. Chem., Int. Ed.*, 2002, **41**, 2790.
25 F. Diederich and R. L. Whetten, *Acc. Chem. Res.*, 1992, **25**, 119.
26 K. Kikuchi, N. Nakahara, T. Wakabayashi, S. Suzuki, H. Shinomori, Y. Miyake, K. Saito, I. Ikemoto, M. Kainosho and Y. Achiba, *Nature*, 1992, **357**, 142.
27 M. Zheng, A. Jagota, M. S. Strano, A. P. Santos, P. Barone, S. G. Chou, B. A. Diner, M. S. Dresselhaus, R. S. Mclean, G. B. Onoa, G. G. Samsonidze, E. D. Semke, M. Usrey and D. J. Walls, *Science*, 2003, **302**, 1545.
28 Y. Shoji, K. Tashiro and T. Aida, *J. Am. Chem. Soc.*, 2006, **128**, 10690.
29 C. Yamamoto, T. Hayashi, Y. Okamoto, S. Ohkubo and T. Kato, *Chem. Commun.*, 2001, 925.
30 R. Kessinger, J. Crassous, A. Herrmann, M. Rüttimann, L. Echegoyen and F. Diederich, *Angew. Chem., Int. Ed.*, 1998, **37**, 1919.
31 N. S. Sariciftci, L. Smilowitz, A. J. Heeger and F. Wudl, *Science*, 1992, **258**, 1474.
32 K. L. Wooley, C. J. Hawker, J. M. J. Fréchet, F. Wudl, G. Srdanov, S. Shi, C. Li and M. Kao, *J. Am. Chem. Soc.*, 1993, **115**, 9836.
33 T. Nishioka, K. Tashiro, T. Aida, J.-Y. Zheng, K. Kinbara, K. Saigo, S. Sakamoto and K. Yamaguchi, *Macromolecules*, 2000, **33**, 9182.
34 T. Yamaguchi, N. Ishii, K. Tashiro and T. Aida, *J. Am. Chem. Soc.*, 2003, **125**, 13934.
35 O. Vostrowsky and A. Hirsch, *Angew. Chem., Int. Ed.*, 2004, **43**, 2326 and references therein.